Interactions of the two heads of scallop (*Argopecten irradians*) heavy meromyosin with actin: influence of calcium and nucleotides

Miklos NYITRAI*†, Andrew G. SZENT-GYÖRGYI‡ and Michael A. GEEVES*[1]

*Department of Biosciences, University of Kent at Canterbury, Canterbury, Kent CT2 7NJ, U.K., †Research Group for Fluorescence Spectroscopy, Office for Academy Research Groups Attached to Universities and Other Institutions, Department of Biophysics, Faculty of Medicine, University of Pécs, P.O.B. 99, H-7601 Pécs, Hungary, and ‡Rosenstiel Basic Medical Sciences Research Center, Brandeis University, Waltham, MA, 02454-9110, U.S.A.

We recently proposed a co-operative model for the influence of calcium and ADP on scallop (*Argopecten irradians*) muscle heavy meromyosin (scHMM), in which scHMM exists in two conformations (designated 'off' and 'on'), and calcium and ADP are allosteric effectors of the equilibrium between the off and on conformations [Nyitrai, Szent-Gyorgyi and Geeves (2002) Biochem. J. **365**, 19–30]. Here we examine the influence of actin on scHMM. In the absence of nucleotide, both heads of scHMM bind very tightly to actin, independent of the presence of calcium. In the absence of calcium, ADP dissociates scHMM from actin completely, and little evidence of ternary complex formation can be found (actin affinity $> 20\ \mu$M). The off state of scHMM therefore does not interact with actin. In the presence of calcium, ADP and actin lower each other's affinity for scHMM by 30–50-fold, although both heads remain strongly attached to actin (actin affinity $0.17\ \mu$M). Detailed analysis suggests that the second head contributes far more to the overall binding energy than is the case for mammalian skeletal muscle HMM. This is consistent with a different stereochemical relationship between the two heads in scallop and mammalian HMM molecules.

Key words: ATPase activity, calcium regulation, enzyme kinetics, myosin, rapid kinetic methods.

INTRODUCTION

The interaction of actin with myosin provides the structural and functional basis for muscle contraction [1]. The contraction of the striated muscle of most animals is regulated by tropomyosin and the troponin complex [2], which are part of the thin filament. In smooth muscle and molluscan muscles, regulation occurs via the myosin light chains, which form the neck of the myosin motor. Regulation involves either phosphorylation of the light chains (smooth muscle myosin) or calcium binding to the light chains [scallop (*Argopecten irradians*) myosin]. Despite the difference in the signalling pathways, the mechanism of regulation via the light chains shows several similarities in the two systems. Many non-muscle myosins have up to six calmodulin-like light chains associated with the myosin neck. The role of calcium binding to these light chains of the non-muscle myosins is not yet clear. A clearer understanding of the regulatory mechanism of scallop muscle myosin may shed light on the regulatory mechanism of both smooth muscle and the non-muscle myosins.

The binding of calcium to molluscan myosin or to its double-headed proteolytic fragment, heavy meromyosin (HMM), increases the Mg-ATPase activity by a factor of ~ 100 in the absence of actin, and by even more in the presence of actin [3,4]. The ATPase activity of the single-headed fragment, myosin subfragment 1 (S1), is not affected by calcium [5], which suggests that the intact junction between the two heads is required for proper regulation. The calcium activation of scallop myosin or scallop HMM (scHMM) ATPase activity occurs in a co-operative manner [6]. Equilibrium experiments have shown that, in the presence of ADP, the binding of calcium to scHMM was co-operative [5]. The binding of calcium to scHMM in the absence of ADP, or the binding of ADP (with or without calcium), did not show co-operativity [5]. We recently proposed [7] a co-operative model for scHMM regulation based on transient kinetic studies of calcium and nucleotide binding to scHMM [8–10]. We proposed that the scHMM exists in two conformations, 'on' and 'off' [7], and that nucleotides and calcium are allosteric effectors that control the equilibrium between the on and off conformations. Calcium favours the on conformation, while ADP favours the off-state.

Little is known in detail about the interaction of molluscan HMM with actin. Previous studies have shown that the simultaneous binding of the two heads of HMM to actin can induce strain in the complex, and this is most apparent in the presence of ADP. This has been documented for both skeletal muscle HMM [11] and unphosphorylated smooth muscle HMM [12]. One curious result was that, for smooth muscle HMM, the strain was less apparent for phosphorylated HMM, suggesting that one role of phosphorylation could be to modulate the strain between the two heads in the presence of actin. We therefore considered that the same phenomenon may be apparent in the calcium regulation of scHMM. In the present work, we studied the effects of nucleotides and calcium on the binding of scHMM to actin by using rapid kinetic stopped-flow methods. The results show that both heads of scHMM interact very strongly with actin in the rigor state, independent of the presence of calcium. In the absence of calcium and the presence of ADP there was little evidence for the binding of scHMM to actin. In the presence of calcium the binding of ADP and actin lowered each other's affinity for scHMM reciprocally by ~ 30-fold. In addition, the

Abbreviations used: mant, 2′(3)-*O*-(*N*-methylanthraniloy); pyr-actin, pyrene-labelled actin; scHMM, heavy meromyosin from scallop (*Argopecten irradians*) striated muscle; S1, myosin subfragment 1; $[X]_F$, concentration of X established after mixing the reactants in the stopped-flow apparatus; $[X]_I$, concentration of X established before mixing the reactants in the stopped-flow apparatus (initial concentration).

[1] To whom correspondence should be addressed (e-mail m.a.geeves@ukc.ac.uk).

second head appears to contribute more to the overall binding than is the case for mammalian skeletal muscle myosin.

MATERIALS AND METHODS

Protein preparations

scHMM was obtained from scallop (*Argopecten irradians*) striated muscle myosin as described previously [13]. scHMM preparations were stored at −80 °C. Thawing was rapid, by placing the vials into a 20 °C water bath. Determination of the Mg-ATPase activity and the calcium sensitivity of the activity using the coupled pyruvate kinase/lactate dehydrogenase assay [5] showed that the preparations retained ATPase activity and calcium sensitivity. In the absence of actin, the turnover rate per scHMM head was in the range 0.32–30.36 s^{-1} in the presence of calcium, and the calcium sensitivity [$(ATPase^{+Ca} - ATPase^{-Ca}) \times 100/ATPase^{+Ca}$] of the preparations was between 85% and 92%. Note that the scHMM concentration is given as the concentration of scHMM heads throughout the paper.

Rabbit skeletal actin was used in most of the experiments described. It was prepared as described previously [14] and labelled with pyrene according to [15]. For a few control experiments, we used actin prepared from scallop striated adductor muscle. The acetone dried powder was obtained from muscles stored in ethylene glycol [6]. The muscles were rinsed and blended for 2 s in 40 mM NaCl, 10 mM Mops and 1 mM $MgCl_2$, pH 7.0. The residue collected by centrifugation (5000 ***g*** for 10 min) was extracted for 5 min with 0.1 M KCl, 0.15 M potassium phosphate, 3 mM MgATP and 0.5 mM dithiothreitol, pH 6.5, followed by 5 × 1 min washes with 0.05 M $NaHCO_3$/1 mM EDTA, pH 7, and then with distilled water in the cold, before extraction with acetone. Scallop actin was prepared from acetone-dried powder using a procedure similar to that for skeletal muscle actin [14], and was used without fluorescence labelling.

Kinetic experiments

Kinetic experiments were carried out at 20 °C in a standard buffer of 20 mM Mops, pH 7.0, 100 mM KCl and 5 mM $MgCl_2$, unless stated otherwise. The buffers also contained 100 μM EGTA or 100 μM $CaCl_2$. The ADP was incubated with 1 unit/ml hexokinase, 2 mM glucose and 50 μM P^1,P^5-diadenosine 5′-pentaphosphate before the experiments to lower ATP contamination. Changes in fluorescence were measured with a standard Hi-Tech SF-61 DX2 stopped-flow spectrophotometer. All the transients shown are the average of between three and six shots of the stopped-flow apparatus. Mant [2′(3)-*O*-(*N*-methylanthraniloy)] and pyrene fluorescence was excited at 365 nm using a 75 W Xe/Hg lamp and monochromator. Fluorescence emission was monitored through a KV 389 cut-off filter.

The concentrations used to describe the experimental conditions throughout the text are the final concentrations ($[X]_F$), established after mixing the reactants in the stopped-flow apparatus (dilution by two; 1:1 mixing). These are the concentrations appropriate to define the rates of the observed reaction. In some experiments the measured amplitudes are characteristic of the equilibrium concentrations of reactants established before mixing. Therefore the Figures presenting data from these experiments (Figures 2, 4c, 5 and 6) show the reactant concentrations before mixing (the initial concentration, $[X]_I$). To avoid confusion, each concentration is labelled in the Figures as $[X]_I$ or $[X]_F$ as appropriate. The scHMM concentration is given as the concentration of scHMM heads.

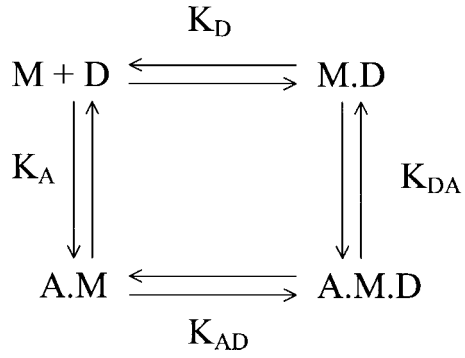

Scheme 1 Coupling between nucleotide and actin binding sites

M, A and D symbolize myosin (or its fragment), actin and ADP respectively. The affinity of the myosin for actin is characterized by K_A in the absence of nucleotide and by K_{DA} in the presence of it. The affinity of myosin for ADP is given by K_D and K_{AD} in the absence and presence of actin respectively. K_A, K_D, K_{DA} and K_{AD} are dissociation equilibrium constants.

Analysis of kinetic and equilibrium results

Fluorescence transients were analysed by fitting to one or two exponential terms as appropriate:

$$F_t = \Delta F \cdot \exp(-k_{obs} \cdot t) + F_\infty \quad (1a)$$

$$F_t = \Delta F_1 \cdot \exp(\pm k_{obs1} \cdot t) + \Delta F_2 \cdot \exp(-k_{obs2} \cdot t) + F \quad (1b)$$

where F_t is the fluorescence at time t, F_∞ is the fluorescence at the end of the reaction, ΔF is the amplitude of the fluorescence change, and k_{obs} is the observed exponential rate constant.

When the complex of pyrene-labelled actin (pyr-actin) and scHMM was dissociated by ATP in the presence of ADP (see Figure 4b), the analysis of the measured k_{obs} values was carried out by using the following equation:

$$k_{obs}/k_0 = 1/\{1 + ([ADP]/K_{AD})\} \quad (2)$$

where k_0 is k_{obs} measured in the absence of ADP, and K_{AD} is the dissociation equilibrium constant for the binding of ADP to pyr-actin–scHMM (Scheme 1).

The equilibrium between bound and free myosin in the presence of actin is defined by the protein concentrations:

$$K = [A]_{free} \cdot [M]_{free}/[AM] \quad (3)$$

where K is the dissociation equilibrium constant for myosin binding to actin, $[A]_{free}$ and $[M]_{free}$ are the free concentrations of actin and myosin respectively, and [AM] is the concentration of the actin–myosin complex. According to Scheme 1, the subscript of K indicates whether the affinity is in the absence (K_A) or presence (K_{DA}) of saturating ADP.

If actin at a fixed concentration is titrated with myosin (see Figures 2 and 5a), the following equation can be used to analyse the measured amplitudes [16]:

$$[A]_0 \cdot S^2 - S \cdot ([A]_0 + [M]_0 + K) + [M]_0 = 0 \quad (4)$$

where $[M]_0$ and $[A]_0$ are the total myosin and actin concentrations respectively, and S is the fraction of myosin bound ($[AM]/[A]_0$). Upon dissociation of the pyr-actin–myosin complex, the change in pyrene fluorescence is proportional to [AM].

In some cases, titrations in the presence of ADP suggested the occurrence of a 'parking problem' – reduced apparent binding at high saturation of actin with HMM because of the reduced availability of pairs of actin sites to bind the dimeric HMM. In

$$A_2 + HMM \underset{}{\overset{K_a}{\rightleftharpoons}} A_2 \text{ - } HMM \underset{}{\overset{K_b}{\rightleftharpoons}} A_2 = HMM$$

one head bound; both heads bound

Scheme 2 Model of the actin–HMM interaction

The Scheme describes the two-step model for the interaction of HMM with actin (A_2). K_a and K_b are the association equilibrium constants attributed to the binding of the first and second head respectively. See [11] for further details.

order to deal with the parking problem, the experiment was performed with actin in excess of HMM at a fixed ratio of $[A]_0/[M]_0$. It is assumed that, in the absence of ADP and at the protein concentrations used here, all HMM heads bind to actin, and therefore the ratio of amplitudes (S) in the presence and absence of ADP defines:

$$S = A/A_{max} = [AMD]/[M]_0 \quad (5)$$

where [AMD] is the concentration of the actin-myosin·ADP complex.

Using the conservation of mass equations and eqn. (3), it can be shown that:

$$[M]_0/K = S/[(1-S)\cdot(\alpha - S)] \quad (6)$$

where α is defined as the ratio of the actin concentration to the myosin concentration ($[A]_0/[M]_0$).

The interpretation of affinity constants for the binding of HMM to actin is dependent upon the structural model used. Here we used the scheme for HMM binding to a pair of actin sites as described by Conibear and Geeves [11], based on the model of Goody and Holmes [17]. Scheme 2 shows the two-step binding model, where the binding of the first of the scHMM heads to actin occurs in a second-order step as for a single-headed fragment. This is followed by the binding of the second head in a first-order process. The association equilibrium constants for the first (K_a) and second (K_b) steps are related to the binding constant for a single-headed S1 (K_S) by:

$$K_a = 4K_S \quad (7a)$$

$$K_b = K_S C/2 \quad (7b)$$

where 4 and 1/2 are statistical terms, and C is the effective actin concentration that is available to the second head. On the basis of geometrical arguments, Goody and Holmes [17] estimated the value of C to be $\sim 100\ \mu$M, and the measurements of Conibear and Geeves for rabbit skeletal proteins were consistent with this value [11]. The affinity of scHMM for actin (K_H) is $K_a \cdot (1+K_b)$, and the following relationship holds:

$$K_H = 2K_S \cdot (2 + K_S \cdot C) \quad (8)$$

To determine the affinities of HMM and S1 for scallop actin, competitive titration experiments were carried out against rabbit pyr-actin, as described previously [16]. The amplitude of the change in pyrene fluorescence was used to calculate the fraction of pyr-actin bound to myosin in the presence of increasing concentrations of unlabelled scallop actin. The analysis of the amplitude data was carried out using least-squares iterative fit with the software Scientist (Micromath, Salt Lake City, UT, U.S.A.). The kinetic model for the fit was created based upon the definition of affinities of myosin for rabbit pyr-actin (K_A*) and unlabelled scallop actin (K_A):

$$K_A^* = [A^*][M]/[A^*M] \quad (9a)$$

$$K_A = [A][M]/[AM] \quad (9b)$$

and the conservation of mass equations:

$$[A^*]_0 = [A^*] + [A^*M] \quad (10a)$$

$$[A]_0 = [A] + [AM] \quad (10b)$$

$$[M]_0 = [M] + [AM] + [A^*M] \quad (10c)$$

where [A], [A*] and [M] are the concentrations of free unlabelled scallop actin, pyr-actin and myosin respectively, while $[A]_0$, $[A^*]_0$ and $[M]_0$ are their total concentrations respectively. [A*M] and [AM] are the concentrations of acto–myosin complexes formed between myosin and rabbit pyr-actin or unlabelled scallop actin respectively.

RESULTS

scHMM characterization by single-turnover experiments

The ATPase rate of scHMM was measured in a single-turnover assay [7,10]. scHMM (0.5 μM) was mixed in a double mixing

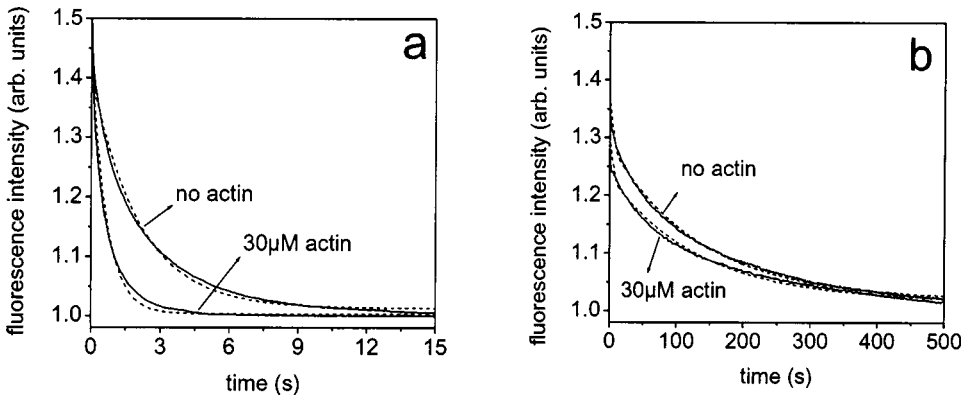

Figure 1 Fluorescence transients recorded in single-turnover ATPase experiments

After aging scHMM (0.5 μM) in a double mixing stopped-flow system for 1 s with 5 μM mant-ATP, the solution was mixed with a large excess of ATP (400 μM) in the presence or absence of 30 μM actin. (**a**) Mant fluorescence transients obtained in the presence of calcium with single-exponential fits superimposed (dashed lines). The k_{obs} values were 0.48 s^{-1} in the absence and 1.51 s^{-1} in the presence of actin. (**b**) Mant fluorescence transients obtained in the absence of calcium with fits to two exponentials superimposed. In the absence of actin, k_{obs} values were 0.44 s^{-1} and 0.007 s^{-1}, with amplitudes of 0.09 and 0.31 arbitrary (arb.) units respectively. In the presence of actin, the k_{obs} values were 0.077 s^{-1} and 0.007 s^{-1}, with amplitudes of 0.07 and 0.22 units respectively. Experimental conditions were 20 mM Mops, pH 7.0, 5 mM $MgCl_2$ and 100 mM KCl, at 20 °C, and either 100 μM EGTA or 100 μM $CaCl_2$. The scHMM concentration is given as the concentration of scHMM heads.

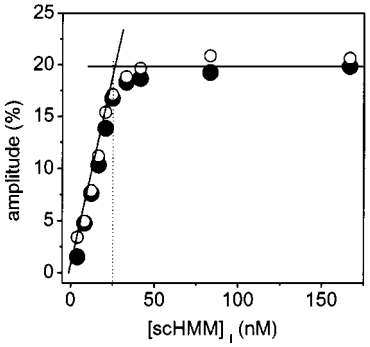

Figure 2 Affinity of scHMM for pyr-actin in the absence of ADP

scHMM (2.5–85 nM) and 12.5 nM pyr-actin were mixed with 15 μM ATP and the pyrene fluorescence was monitored. The amplitude of the observed fluorescence changes in the presence (●) or absence (○) of calcium is shown plotted against [scHMM]. [scHMM] is that established before mixing, as indicated by the subscript. Hyperbolae fits gave affinities (K_A) of 1.3 nM and 1.4 nM in the presence and absence of calcium respectively. Saturation of the amplitude occurred at a stoichiometry of two actins per scHMM (dotted line). Conditions were as in Figure 1.

stopped-flow system with 5 μM mant-ATP and aged for 1 s to allow saturation of the protein with mant-ATP. The reactants were then mixed with a large excess of unlabelled ATP (400 μM) to displace the bound mant-labelled nucleotide. Figure 1 shows the fluorescence transients recorded in the presence (Figure 1a) and absence (Figure 1b) of calcium. In the presence of calcium, the transients were analysed as a single exponential. In the absence of actin the k_{obs} was 0.3–0.5 s^{-1} at 100 mM KCl, in agreement with our previous results [7]. When 30 μM actin was premixed with the ATP (400 μM) before mixing with scHMM in the stopped-flow apparatus, k_{obs} increased 3–4-fold to 1.2–1.6 s^{-1}. In the absence of calcium, the fluorescence traces were double exponential (Figure 1b). The fast phase had k_{obs} values of 0.4–0.6 s^{-1} and 0.7–1.5 s^{-1} in the absence and presence of actin (30 μM) respectively, and contributed approx. 20 % to the total fluorescence change. This phase was attributed to the unregulated fraction of the scHMM heads that behave like HMM in the presence of Ca^{2+}. The slow phase was characterized by k_{obs} = 0.006–0.008 s^{-1}, and was not accelerated by actin (30 μM).

Interaction of scHMM with pyr-actin in the rigor complex

The binding of myosin heads to pyr-actin in the strongly bound rigor-like complex quenches the fluorescence of the pyrene group by up to ~ 70 %. This signal can therefore be used to assess the fraction of myosin heads bound tightly to actin. In the case of HMM this is important, because there may be steric constraints on the two heads binding simultaneously to two adjacent actin sites. A simple and accurate way to assess the fraction of actin sites occupied by myosin is to incubate HMM and actin together to form a stable complex, and then to measure the fluorescence amplitude following the ATP-induced dissociation of myosin from the complex. When 12.5 nM pyr-actin and various concentrations of scHMM (2.5–85 nM) were dissociated by the addition of 15 μM ATP, the increase in pyrene fluorescence could be described by a single exponential, and k_{obs} (33–35 s^{-1}) was independent of the scHMM concentration and the presence of calcium. Figure 2 shows the dependence of the measured amplitudes on the scHMM concentration. The concentrations shown in Figure 2 are those established before the stopped-flow shots. The amplitudes increased linearly up to the break point, and were then constant. The break point occurred at 25 nM scHMM, i.e. at a 1:1 stoichiometry of HMM heads to actin, and the position and signal amplitude at the break were independent of calcium. This indicates that, in the rigor scHMM–pyr-actin complex, both of the heads bind to actin very tightly, and each head makes a similar contribution to the quenching of the pyrene fluorescence. Hyperbolae fits to the data gave affinities (K_A) of 1.3 nM and 1.4 nM in the presence and absence of calcium respectively. Although the precise determination of K_A is difficult in these experiments, due to the very tight binding, the values determined from the hyperbolae fits, together with the shape of the break-point titration, indicate that the affinity of HMM for actin is < 5 nM. The affinity of S1 under similar conditions was 440 nM [18], suggesting that the second head makes a significant contribution to the binding energy.

The kinetics of the ATP-induced dissociation of scHMM from actin are shown in Figure 3. Mixing 100 nM pyr-actin and 50 nM scHMM with excess ATP (5–30 μM) resulted in a fluorescence

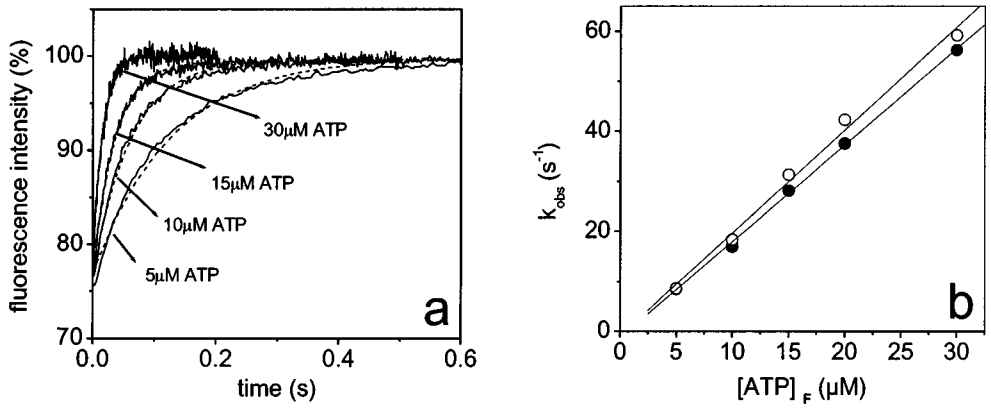

Figure 3 Dissociation of actin from pyr-actin–scHMM by ATP

scHMM (50 nM) and pyr-actin (100 nM) were mixed with ATP (5–30 μM) in the presence or absence of calcium. (**a**) Pyrene fluorescence transients observed in the presence of calcium with [ATP] as indicated. Single-exponential functions fitted to the transients are superimposed (dashed lines). (**b**) Measured k_{obs} values as a function of [ATP] in the presence (●) and absence (○) of calcium. The second-order rate constants (K_1k_{+2}) from linear fits are 1.95×10^6 $M^{-1} \cdot s^{-1}$ and 2.05×10^6 $M^{-1} \cdot s^{-1}$ in the presence and absence of calcium respectively.

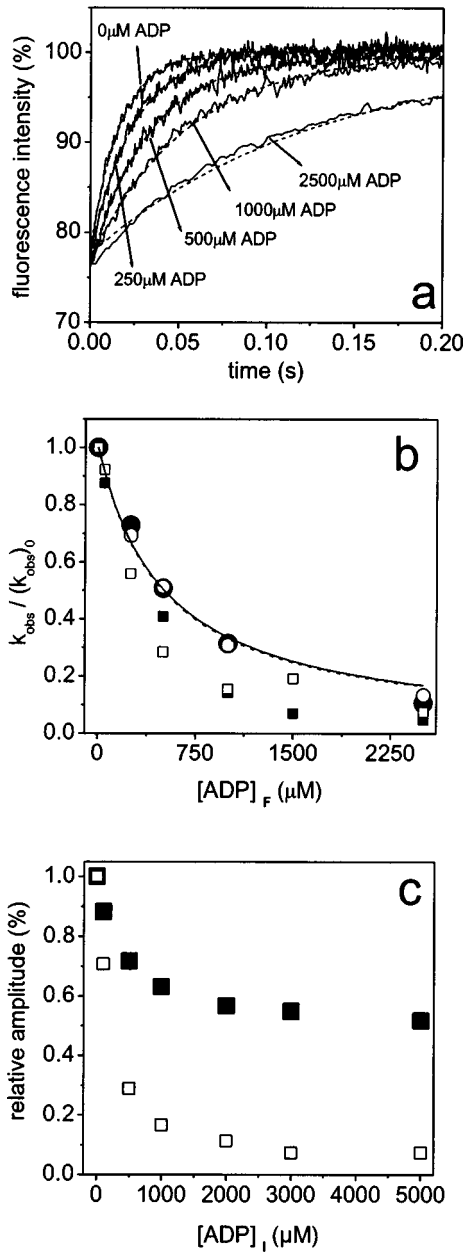

Figure 4 Inhibition by ADP of the ATP-induced dissociation of the scHMM–pyr-actin complex

scHMM (50 nM) and pyr-actin (100 nM) were mixed with 30 μM ATP and ADP (0–2500 μM) in either the presence or the absence of calcium. (**a**) Pyrene fluorescence traces recorded when ADP at various concentrations was preincubated with ATP in the absence of calcium, with single-exponential fits superimposed (dashed lines). (**b**) ADP-concentration-dependence of relative k_{obs}, defined as k_{obs}/k_0 in the presence (●) and absence (○) of calcium. k_{obs} data were fitted to eqn. 2 (solid and dashed lines), and $K_{AD} = 500 \pm 40$ μM, independent of the presence of calcium. The experiments were also carried out by preincubating the pyr-actin–scHMM complex with ADP before mixing it with ATP. The ADP-concentration-dependence of relative k_{obs} measured in the presence (■) or absence (□) of calcium is also shown. (**c**) ADP-concentration-dependence of the relative amplitudes (defined as the ratio of the measured amplitude to that obtained in the absence of ADP) in the presence (■) or absence (□) of calcium for the case when the protein was preincubated with ADP.

increase of 25%, and the transients were single-exponential and independent of calcium. Figure 3(b) shows the k_{obs} values; linear fits to the k_{obs} against [ATP] plot gave apparent second-order rate constants of 1.95×10^6 $M^{-1} \cdot s^{-1}$ and 2.05×10^6 $M^{-1} \cdot s^{-1}$ in the presence and absence of calcium respectively. A similar second-order rate constant (2.5×10^6 $M^{-1} \cdot s^{-1}$) was found for scallop S1 [18].

Inhibition by ADP of the ATP-induced dissociation of the scHMM–pyr-actin complex

If ADP binds rapidly and weakly to acto-scHMM, its affinity can be estimated from the inhibition of the rate of the ATP-induced dissociation of the actin–scHMM complex. If the reaction is a rapid equilibrium, then k_{obs} values when ADP is preincubated with the protein or with the ATP should be identical. The dissociation of 50 nM scHMM and 100 nM pyr-actin by 30 μM ATP with ADP premixed in the ATP is shown in Figure 4(a). The amplitude was independent of [ADP], but the k_{obs} value decreased with increasing [ADP]. Figure 4(b) shows the analysis of the k_{obs} values, and demonstrates that the results are independent of the presence of calcium. Similar results for k_{obs} were found if the proteins (rather than the ATP) were preincubated with ADP. Analysis of the curves in Figure 4(b) according to eqn. (2) gives a value of $K_{AD} = 500 \pm 40$ μM.

In the experiment when ADP was preincubated with the proteins, the amplitude decreased with increasing [ADP] (Figure 4c), indicating that ADP weakens the affinity of scHMM for pyr-actin. Note that Figure 4(c) presents the ADP concentrations before mixing, as the measured amplitudes are characteristic of the scHMM–pyr-actin complex formed in the equilibrium before the stopped-flow shots. In the presence of calcium and 5 mM ADP, the amplitude decreased to approximately half of its value measured in the absence of ADP. Accordingly, half of the scHMM–pyr-actin complexes were dissociated at this [ADP]. K_{DA} can be estimated from eqn. (3), giving a value of ~ 150 nM. In the absence of calcium, the amplitude decreased to $\sim 10\%$ of its value measured in the absence of ADP, which shows that ADP dissociated scHMM from pyr-actin almost completely, consistent with $K_{DA} \gg 150$ nM.

Affinity of scHMM for pyr-actin in the presence of ADP

To determine the value of K_{DA} (Scheme 1), the experiment of Figure 2 was repeated in the presence of ADP. Figure 5(a) shows the measured amplitude when the mixture of 50 nM pyr-actin, 1.5 mM ADP and various scHMM concentrations was dissociated by 100 μM ATP. The dashed line indicates the best fit of a hyperbolic curve to the data (eqn. 4), which gave maximum amplitude of 18.3%. This deviates from the measured data points but, more significantly for the data shown, fails to reproduce the maximum predicted amplitude (22.5%) of the reaction (dotted line in Figure 5a), based on the results of experiments carried out in the absence of ADP. A similar deviation of the best-fit hyperbola was observed using a pyr-actin concentration of 12.5 nM or 150 nM. A possible explanation for the poor fit of data to the hyperbola is the 'parking problem' [19,20], whereby, as saturation approaches, the number of available pairs of actin sites becomes restricted and less scHMM binds than would have been predicted. To address this problem, we developed a novel titration strategy in which the ratio of actin sites to scHMM heads was kept constant as the total protein concentration was varied. As the total protein concentration increased, the fraction of the protein present as acto-HMM increased. The amplitude data were analysed using eqn. (6). The value of S was determined experimentally by comparing the pyrene fluorescence amplitudes with those obtained in the absence of ADP, i.e. when practically all of the heads were bound to actin ($K_A < 5$ nM). Figure 5(b) shows the value of S as a function of

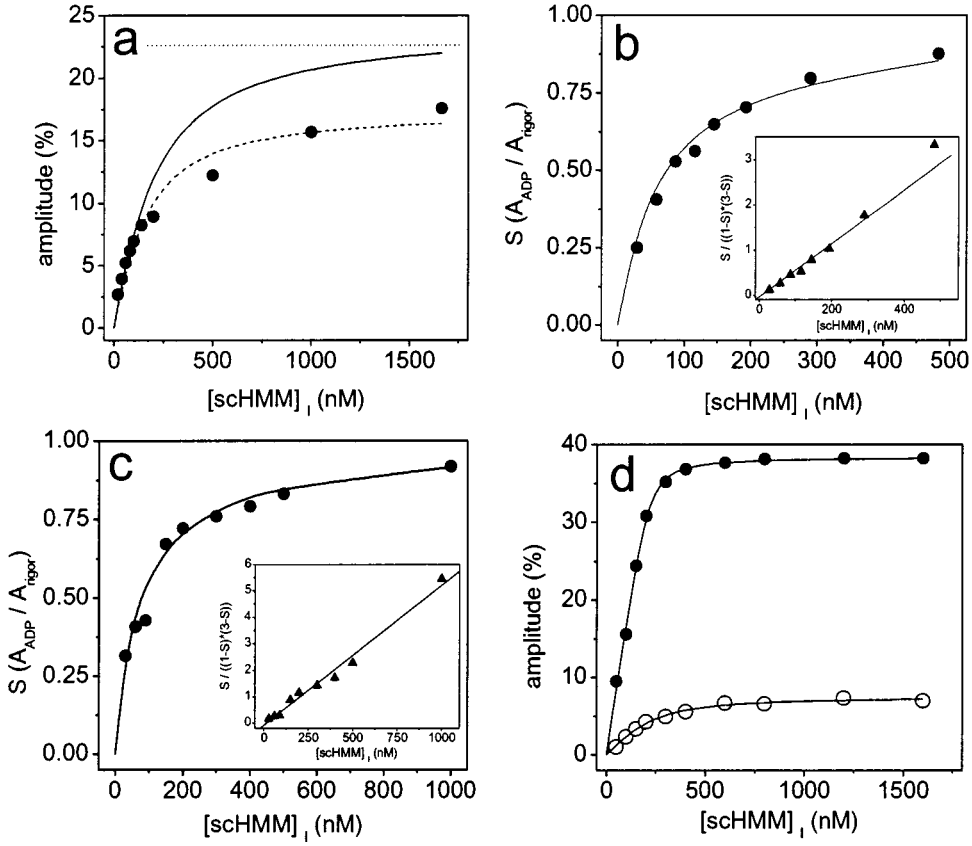

Figure 5 Affinity of scHMM for pyr-actin in the presence of ADP

(**a**) Titration of 50 nM pyr-actin with scHMM, as in Figure 2 but in the presence of 1.5 mM ADP and 100 μM calcium. The dashed line shows the best-fit hyperbola; $K_{DA} = 105 \pm 23$ nM with a maximum amplitude of 18.3%. The solid line assumes $K_{DA} = 170$ nM and maximum predicted amplitude (A_{max}) = 22.5% (A_{max} is shown as a dotted line; see the text). (**b**) Similar experiment to (**a**), but with the [pyr-actin]/[scHMM] ratio fixed at 3. The solid line assumes $K_{DA} = 170$ nM. The inset was created using eqn. (6), and a linear fit gives $K_{DA} = 170 \pm 10$ nM. (**c**) Similar experiment to (**b**), but at 2.5 mM ADP. The linear fit with eqn. (6) (inset) revealed $K_{DA} = 189 \pm 8$ nM. (**d**) Results of experiments carried out at 30 mM KCl in the presence (●) and absence (○) of calcium. Various concentrations of scHMM, 100 nM pyr-actin and 1.5 mM ADP were mixed with 100 μM ATP. The scHMM-concentration-dependence of the measured amplitude was fitted to hyperbolae, with $K_{DA} = 12.6 \pm 2.2$ nM and 74 ± 29 nM in the presence and absence of calcium respectively. scHMM concentrations shown are those established before mixing, as indicated by the subscript. All other conditions were as in Figure 2.

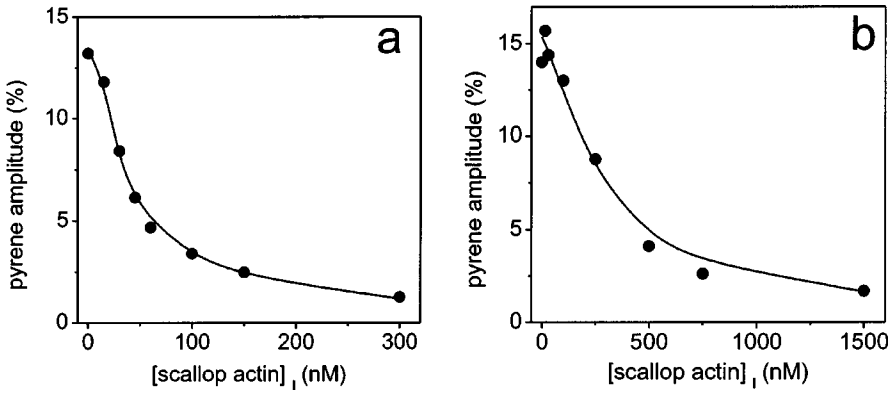

Figure 6 Affinity of skeletal S1 and scHMM for scallop actin

(**a**) Rabbit pyr-actin (30 nM) was incubated with 30 nM scHMM and various concentrations of scallop actin, and then mixed with 10 μM ATP. Amplitudes were measured during the dissociation of scHMM from pyr-actin. The best fit to the competitive binding isotherm (eqns. 9 and 10) is shown superimposed, and gives the affinity of rabbit pyr-actin as 10.2 ± 1.3 nM and that of scallop actin as 5.3 ± 0.7 nM. (**b**) Similar experiment using 30 nM rabbit pyr-actin and 150 nM rabbit skeletal muscle S1 titrated with scallop actin. The affinity of S1 was 52.5 ± 5.3 nM for rabbit pyr-actin and 41.2 ± 8.7 nM for scallop actin. The scallop actin concentration shown is that established before mixing, as indicated by the subscript. The experiments were carried out in 20 mM Mops, pH 7.0, 100 mM KCl and 5 mM $MgCl_2$.

[scHMM] from experiments in which the ratio of [pyr-actin] to [scHMM], α, was 3. [scHMM] given in the Figure is that established before the stopped-flow shots. The plots of $S/[(1-S)\cdot(\alpha-S)]$ against [scHMM] were linear, and the slope of the fit was used to calculate the value of K_{DA} (inset of Figure 5b). According to the fit, the value of K_{DA} was 170 ± 10 nM. Measurement at $\alpha=2$ or 5 gave similar values of K_{DA} (170–180 nM), although the errors in the amplitude measurements become large as α increases. Using a value of K_{DA} of 170 nM, the predicted curve for Figure 5(a) is shown as a solid curve. This fits the data reasonably well for [scHMM] up to 100 nM or 50% saturation of the actin, but subsequently predicts more binding than was observed. This is consistent with the parking problem causing reduced binding at high saturation. The experiment was repeated at [ADP] = 2.5 mM (Figure 5c) and the value of K_{DA} was determined to be 189 ± 8 nM, indicating that the increase in the ADP concentration from 1.5 to 2.5 mM had little effect on the measured affinity of scHMM for actin.

Similar affinity experiments in the absence of calcium were not possible because of very weak binding of scHMM to actin. To address this problem, the measurements were repeated at the lower ionic strength of 30 mM KCl. Pyr-actin (100 nM) was equilibrated with scHMM (25 nM and 850 nM) in the presence of 1.5 mM ADP, then mixed with 100 μM ATP. Analysis of the measured pyrene fluorescence transients resolved k_{obs} values in the range 35–45 s^{-1}, independent of the presence of calcium and of the protein concentration. Figure 5(d) shows the dependence on [scHMM] of the measured amplitudes. The concentrations on the x-axis are those established before mixing. In the presence of calcium, the amplitude increased to $\sim 38\%$, which is close to the value obtained in the absence of ADP in control experiments (42%). Accordingly, in the presence of calcium more than 90% of the scHMM heads were bound to pyr-actin at 1700 nM scHMM in the presence of ADP, reflecting the tight binding of scHMM to pyr-actin (K_{DA} ~ 10 nM). In the absence of calcium the maximum amplitude of the change in pyrene fluorescence was only 7.5% (Figure 5d), which is $\sim 20\%$ of that measured in the presence of calcium and attributed to the unregulated scHMM fraction. All of these observations show that, in the presence of ADP and the absence of calcium, the binding of scHMM to pyr-actin is very weak.

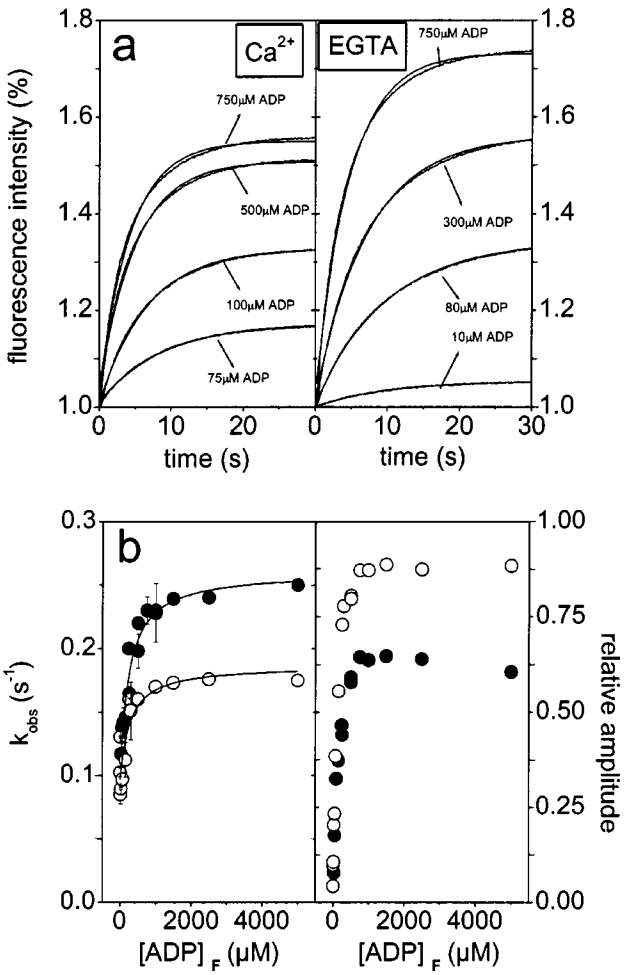

Figure 7 Dissociation of the scHMM–pyr-actin complex by ADP

scHMM (50 nM) and pyr-actin (100 nM) were mixed with ADP (2–5000 μM). (**a**) Pyrene fluorescence transients measured in the presence (left panel) or absence (right panel) of calcium at various ADP concentrations as indicated, with single-exponential fits superimposed. (**b**) k_{obs} and relative amplitude (the ratio of the measured amplitude to that obtained by dissociating the rigor pyr-actin–scHMM complex with ATP) values plotted as a function of [ADP] in the presence (●) or absence (○) of calcium. Hyperbola fits to the k_{obs} against [ADP] curves gave a calcium-independent intercept value of 0.1 s^{-1}. In the presence of calcium the maximum k_{obs} was 0.26 s^{-1}, while in its absence the maximum k_{obs} was 0.19 s^{-1}.

Experiments with scallop actin

We considered the possibility that the relatively weak affinities of scHMM and scallop S1 for actin as compared with the affinities of rabbit skeletal muscle HMM and S1 may be due to the fact that we used actin from rabbit skeletal muscle. To explore this possibility, we prepared actin from scallop striated muscle and measured its affinity for S1 and HMM by using a competitive binding assay with rabbit pyr-actin [16]. In the assay, 30 nM rabbit pyr-actin was incubated with 30 nM scHMM and various concentrations of unlabelled scallop actin, then mixed with 10 μM ATP. The amplitudes measured during the dissociation of scHMM from pyrene actin were plotted against the scallop actin concentration (Figure 6a), and the dissociation equilibrium constants were determined by a least-squares fitting procedure using eqns. (9) and (10) [16]. The affinity of scHMM proved to be similar for rabbit pyr-actin (10.2 ± 1.3 nM) and scallop actin (5.3 ± 0.7 nM) in the absence of nucleotides. When 30 nM pyr-actin and 150 nM rabbit S1 were titrated with scallop actin (Figure 6b), the affinity of rabbit S1 was determined to be 52.5 ± 5.3 nM for pyr-actin and 41.2 ± 8.7 nM for scallop actin. Scallop actin has a slightly higher affinity for rabbit S1 than does rabbit pyr-actin, but the value is similar to a previous estimate for unlabelled rabbit actin (34 nM [16]). Similar experiments were carried out using scallop myosin S1. However, due to the weak affinity of scallop S1 for rabbit actin (440 nM [18]), values for scallop actin could not be resolved. The data show that the affinity of scallop S1 for scallop actin cannot be much higher than 440 nM. These observations suggest that the use of actin from skeletal muscle could not account for the relatively weak affinity of scallop myosin for actin.

Dissociation of the scHMM–actin complex by ADP

Since the affinity of scHMM for actin is very low in the presence of ADP, the ADP-induced dissociation of actin–scHMM at low protein concentrations provides an alternative source of information on the ternary complex. Figure 7(a) shows the fluorescence traces obtained by mixing 100 nM pyr-actin and 50 nM scHMM with ADP. The transients were single-exponential in either the presence (Figure 7a, left panel) or the

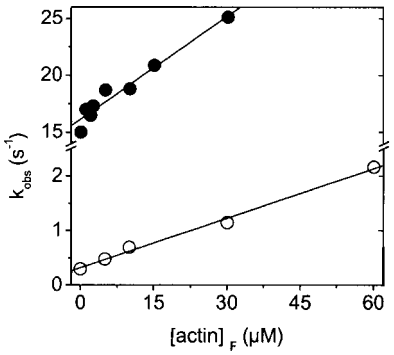

Figure 8 Effect of actin on the dissociation of mant-ADP from scHMM

scHMM (0.5 μM) and mant-ADP (15 μM) were mixed with 300 μM ATP and various concentrations of unlabelled actin (0–60 μM). The change in the fluorescence of mant-ADP was monitored, and was analysed with single-exponential functions. The amplitudes were $\sim$ 4–5%, and were independent of the presence of calcium and actin. The Figure shows the actin-concentration-dependence of k_{obs} measured in the presence (●) or absence (○) of calcium. Linear fits (solid lines) gave second-order rate constants of 0.3×10^6 $M^{-1} \cdot s^{-1}$ and 0.03×10^6 $M^{-1} \cdot s^{-1}$ and intercepts of 16 s^{-1} and 0.3 s^{-1} in the presence and absence of calcium respectively.

absence (Figure 7a, right panel) of calcium. The k_{obs} values were between 0.1 s^{-1} and 0.26 s^{-1}, indicating slow dissociation of the scHMM–pyr-actin complex. Hyperbolic fits to the k_{obs} against [ADP] data (continuous lines in Figure 7b, left panel) indicated that the intercepts of the curves were relatively calcium-independent (0.1 s^{-1}). In the presence of calcium the maximum value for k_{obs} was 0.26 s^{-1}, while that in the absence of calcium was 0.19 s^{-1}. Relative amplitudes were calculated as the ratio of the measured amplitudes to the amplitude obtained by dissociating the pyr-actin–scHMM complex with excess ATP, and are plotted in Figure 7(b). The maximum values of the relative amplitude were $\sim$ 0.6 and $\sim$ 0.9 in the presence and absence respectively of calcium, which suggests that 60% and 90% respectively of the heads were dissociated by ADP. These observations are in agreement with the results of the affinity experiments described above.

Effect of actin on the dissociation of mant-ADP from scHMM

The ability of actin to dissociate ADP from HMM was investigated by measuring the rate at which mant-ADP was displaced by ATP in the presence of increasing concentrations of actin. The rate of mant-ADP release was characterized in our recent work with scHMM in the absence of actin [7]. In this case only one head of HMM binds mant-ADP in the absence of calcium, with an affinity of 1 μM. In the presence of calcium, both heads bind mant-ADP with an affinity of 15 μM. In the present experiments, 0.5 μM scHMM was equilibrated with 15 μM mant-ADP and then mixed with 300 μM ATP and different actin concentrations (up to 60 μM). Apart from the 15–20% unregulated fraction observed in the absence of calcium, the traces were single-exponential and the amplitude was consistent with complete displacement of the bound mant-ADP. Analysis of the single-exponential fluorescence transients indicated that the amplitude of the fluorescence decrease (4–5%) was independent of the actin concentration. The k_{obs} values are plotted as a function of actin concentration in Figure 8. In the presence of calcium, k_{obs} increased from 15 s^{-1} in the absence of actin to 25 s^{-1} in the presence of 30 μM actin. In the absence of calcium, k_{obs} was 0.3 s^{-1} in the absence of actin and increased linearly to $\sim$ 2.2 s^{-1} at 60 μM actin. The data were fitted to a line, and the gradients defined an apparent second-order rate constant of $\sim 0.3 \times 10^6$ $M^{-1} \cdot s^{-1}$ in the presence and $\sim 0.03 \times 10^6$ $M^{-1} \cdot s^{-1}$ in the absence of calcium. Thus it appears that actin can interact with scHMM·ADP in the absence of calcium – at least transiently – to induce displacement of ADP, but that the effective rate of actin binding is ten times greater in the presence of calcium.

Determination of the weakly bound scHMM fraction

For rabbit skeletal muscle proteins, the pyrene fluorescence on pyr-actin specifically monitors the strongly attached myosin heads. Light scattering, in contrast, can measure any attached HMM. The changes in both the light-scattering (Figure 9a) and pyrene fluorescence (Figure 9b) signals were recorded when scHMM (1 μM) and pyr-actin (2 μM) were mixed with ADP (1.5 mM) in the presence of calcium. Both signals were well described by single-exponential fits, and gave amplitude changes

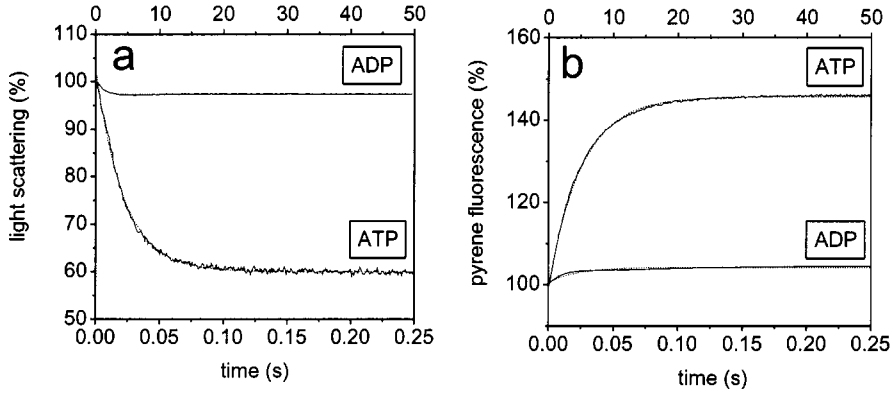

Figure 9 ATP- or ADP-induced dissociation of scHMM from actin, as revealed by pyrene fluorescence or light scattering

scHMM (1 μM) and pyr-actin (2 μM) were mixed with ATP (25 μM) or ADP (1.5 mM) in the presence of calcium (100 μM), and the changes in light scattering (**a**) and pyrene fluorescence (**b**) were monitored. The upper and lower *x*-axes show the time scales corresponding to the traces obtained when the pyr-actin–scHMM complex was dissociated by ADP and ATP respectively. Both signals were well described by single-exponential fits (dashed lines). When the pyr-actin–scHMM complex was mixed with ATP, pyrene fluorescence increased by 46.7%, while light scattering decreased by 41.7%. Mixing with ADP gave a 4.1% increase in pyrene fluorescence and a 3.7% decrease in light scattering.

of 3.7% [light-scattering $\Delta F/(F_\infty + \Delta F)$] and 4.1% [pyrene fluorescence $\Delta F/(F_\infty - \Delta F)$, where ΔF and F_∞ are as in eqn. 1]. The measurement was repeated with ATP (25 μM) to define the total amount of attached and strongly bound heads. During the ATP-induced dissociation of the pyr-actin–scHMM complex, the pyrene fluorescence increased by 46.7%, while the light scattering decreased by 41.7% (calculated as shown above). These values correspond to the complete dissociation of scHMM from actin. Accordingly, addition of ADP resulted in pyrene fluorescence reporting the dissociation of 8.8% of the heads, while the light-scattering signal sensed the detachment of 8.9% of the heads. This suggests that scHMM heads are either strongly attached or detached, with little evidence of any weakly attached heads.

DISCUSSION

In the work presented here, we have attempted to define the influence of calcium and ADP on the interaction of scHMM with actin. The parameters determined are presented in Table 1, along with those obtained previously for scallop S1. In our previous paper [7] we proposed a co-operative allosteric model for the influence of calcium and ADP on scHMM in the absence of actin. In this model scHMM exists in two major states, designated on and off with respect to the Mg^{2+}-ATPase activity. Calcium and ADP are allosteric effectors of the on/off equilibrium position; calcium favours the on conformation, while ADP favours the off conformation.

In the present work, the measured ATPase activities show that, apart from the 20% of scHMM that is unregulated, the system is predominantly off in the absence of calcium and the presence of ATP. Little evidence for activation of the scHMM ATPase by actin was apparent. Thus the steady-state $M \cdot ADP \cdot P_i$ complex is predominantly off, and has no significant interaction with actin.

In contrast, under rigor-like conditions (no nucleotide), scHMM binds very tightly to actin ($K_A < 5$ nM), with a stoichiometry of two actins per scHMM. Both heads interact strongly with actin, as judged by pyrene fluorescence, and both contribute to binding, as shown by the greatly increased affinity of actin for scHMM compared with the single-headed S1 ($K_A = 440$ nM). Calcium has no measurable effect on actin binding under these conditions.

Initial nucleotide binding to actin–HMM also appears to be unaffected by calcium. The rate constant for the ATP-induced dissociation of actin from the complex (K_1k_{+2}) is independent of calcium. The transition to the off conformation must therefore occur after dissociation from actin. Our previous work in the absence of actin indicated that the on/off equilibration was fast (< 10 ms), and that the hydrolysis of ATP to protein-bound $ADP \cdot P_i$ was also fast and independent of the presence of calcium. It is not therefore possible to establish whether the on/off switch precedes or follows the hydrolysis of ATP after dissociation from actin.

In the presence of ADP the situation is more complex. When ADP is in direct competition with ATP for actin–scHMM, its affinity is very weak ($K_{AD} = 500$ μM) and calcium-independent. Thus both nucleotide pockets appear to be accessible to nucleotide in the presence and absence of calcium, and actin traps the scHMM in an on-like conformation. ADP can only induce a very slow change in the actin–scHMM complex (< 0.3 s^{-1}), and this is slower than the rate constant at which a single rigor-like HMM head might be expected to detach from actin. For example, the rate at which S1 dissociates from the actin–S1 complex was estimated as 3.1 s^{-1} [18]. It is therefore possible that ADP only induces a change in the properties of HMM when both heads are detached from actin. The fact that ADP does change the properties of HMM is clear from the ADP-induced > 30-fold reduction in the affinity of actin for HMM in the presence of calcium compared with a > 3000-fold change in its absence.

The affinities of scHMM for actin in the presence of ADP reveal additional interesting observations. In the presence of calcium and ADP, the binding of scHMM to actin shows significant deviations from simple hyperbolic binding. This behaviour may be an example of a 'parking problem' for HMM on actin. If the HMM binds randomly to pairs of adjacent actin sites, then, as saturation of actin approaches, it is expected that single sites will begin to be left vacant. Filling such sites can only be achieved by binding HMM via a single head (with a much weaker affinity) or by allowing time for spontaneous rearrangement of the HMM on the actin surface, which would be a very slow process. Our analysis of binding under conditions where the actin sites always remain in excess of HMM eliminates the parking problem, and provides a realistic estimate for HMM affinity that is consistent with the relationship $K_{AD}/K_A = K_{DA}/K_D$.

Further analysis of the actin binding data using the model of Goody and Holmes [17] and Conibear and Geeves [11] allows an estimate of the contribution of the second head to the binding energy. A significant difference between scHMM and skeletal muscle HMM is that, even in the presence of ADP and calcium, both heads of scHMM bind actin in a tight binding R-state and quench the pyr-actin fluorescence. Under these conditions there is no occupancy of the more weakly bound A-state for scHMM. A simpler binding model is therefore appropriate in which the association constant for HMM is defined by the association constant for a single head (K_S) and the effective actin concentration available to the second head (C) (eqn 8). On the basis of simple geometric arguments, Goody and Holmes suggested that C would be of the order of 100 μM [17], and this was consistent with the estimates of Conibear and Geeves for rabbit skeletal HMM in the presence and absence of ADP [11]. Using the values in Table 1 for K_{DA} of scallop S1 and HMM (equivalent to $1/K_S$ and $1/K_H$ in eqn 8) gives a value of C of 1 mM, i.e. much higher than that expected on geometric arguments. This suggests that the first head restricts the space that the second head can explore and aligns the second head favourably with the adjacent actin site. A similar calculation in the absence of ADP is not possible, because we only have an upper limit of the value of K_H. However, if C were 1 mM, then K_H would be of the order of 0.1 nM, a very high affinity but one that we cannot rule out.

In the absence of calcium, the affinity of actin for $scHMM \cdot ADP$ is similar to that of scallop $S1 \cdot ADP$ or weaker,

Table 1 Kinetic and equilibrium constants characterizing the interaction of scHMM with nucleotides, actin and calcium

Data are from the present study, from [7]* or from [18]†. See the text and Scheme 1 for details.

	scHMM		
Parameter	+ Ca	+ EGTA	Scallop S1†
K_1k_{+2} (ATP) ($10^6 \times M^{-1} \cdot s^{-1}$)	2	2	2.5
K_D (μM)	15*	1*	10
K_{AD} (μM)	500	500	480
K_A (nM)	< 5	< 5	440
K_{DA} (μM)	0.17	> 20	20‡

‡ Calculated on the basis of thermodynamic coupling presented in Scheme 1.

and is therefore consistent with the second head contributing little to the binding energy. The binding is so weak in this case that we have been unable to gain significant evidence of actin binding scHMM·ADP even at low ionic strength. It is likely that the actin binding that we do observe is dominated by the unregulated fraction of scHMM in our sample. Our previous work has shown that, in the absence of calcium and actin, scHMM is predominantly in the off conformation, with only a single site occupied by ADP. This scHMM species therefore has a very low affinity for actin, and even the head with no ADP bound is in a conformation that has a low affinity for actin. This is consistent with our view that calcium and ADP modulate the on–off equilibrium of scHMM as a whole. The heads are not independent. The affinity of scHMM·ADP for actin is so low that it is not possible to address the question of which head of scHMM (the one with or without a tightly bound ADP) is able to interact with actin.

A comparison of scHMM with smooth muscle HMM underlines their similarities and differences. Scallop myosin is a typical fast-muscle myosin; its actin–S1 has very weak affinity for ADP, and actin is very effective at displacing ADP in both thermodynamic ($K_{AD}/K_D = 33$) and kinetic ($k_{-AD}/k_{-D} > 10$) measurements [7,18]. Smooth muscle myosin is characteristic of a muscle designed for slower contraction and more efficient tension maintenance. The actin–S1 has much lower thermodynamic coupling between ADP and actin binding ($K_{AD}/K_D = 4.2$) [21]. These differences are maintained in the on-states of the two HMM species. In the rigor state or in the on-state with ADP, both heads interact with actin and the second head makes a significant contribution to binding. The contribution is smaller in the case of smooth muscle HMM. Smooth muscle HMM binds only 2–3-fold more tightly than a single S1·ADP, compared with 100-fold tighter for scHMM. Thus, in the on state, both heads of the two types of HMM behave like independent motor domains with respect to binding actin and nucleotide.

In summary, we can draw the following conclusions. In the absence of nucleotide, calcium has little influence on actin binding to scHMM. Both ADP and calcium (in the presence of ADP) have a major influence on the interaction of scHMM with actin. In the presence of calcium, ADP and actin have reciprocal effects on each other's affinity; each affinity is reduced by about 30–50-fold. In the absence of calcium there is very little evidence of any ternary complex formation. Thus ADP and actin are almost mutually exclusive in binding to scHMM. This very weak binding to actin is also found with the ADP·P_i complex, and indicates that the off conformation of scHMM does not bind actin. The route between actin–scHMM in rigor and the detached scHMM·ADP off state is very slow, and may require the spontaneous detachment of heads before ADP can induce the off conformation.

We thank Professor Roger Goody for providing us with the mant-nucleotides, and Nancy Adamek and Elizabeth O'Neall-Hennessey for technical support. This work was supported by a Wellcome Trust Programme grant 055841 and a European Union grant HPRN-CT-2000-00091 (to M. A. G.) and by a NIH Grant AR17346 (to C. Cohen).

REFERENCES

1 Geeves, M. A. and Holmes, K. C. (1999) Structural mechanism of muscle contraction. Annu. Rev. Biochem. **68**, 687–728
2 Gordon, A. M., Homsher, E. and Regnier, M. (2000) Regulation of contraction in striated muscle. Physiol. Rev. **80**, 853–924
3 Wells, C. and Bagshaw, C. R. (1985) Calcium regulation of molluscan myosin ATPase in the absence of actin. Nature (London) **313**, 696–697
4 Wells, C. and Bagshaw, C. R. (1984) The Ca^{2+} sensitivity of the actin-activated ATPase of scallop heavy meromyosin. FEBS Lett. **168**, 260–264
5 Kalabokis, V. N. and Szent-Györgyi, A. G. (1997) Cooperativity and regulation of scallop myosin and myosin fragments. Biochemistry **36**, 15834–15840
6 Chantler, P. D., Sellers, J. R. and Szent-Gyorgyi, A. G. (1981) Cooperativity in scallop myosin. Biochemistry **20**, 210–216
7 Nyitrai, M., Szent-Gyorgyi, A. G. and Geeves, M. A. (2002) Kinetic model of the cooperative binding of calcium and ADP to scallop heavy meromyosin. Biochem. J. **365**, 19–30
8 Wells, C., Warriner, K. E. and Bagshaw, C. R. (1985) Fluorescence studies on the nucleotide- and Ca2 + -binding domains of molluscan myosin. Biochem. J. **231**, 31–38
9 Jackson, A. P. and Bagshaw, C. R. (1988) Kinetic trapping of intermediates of the scallop heavy meromyosin adenosine triphosphatase reaction revealed by formycin nucleotides. Biochem. J. **251**, 527–540
10 Jackson, A. P. and Bagshaw, C. R. (1988) Transient-kinetic studies of the adenosine triphosphatase activity of scallop heavy meromyosin. Biochem. J. **251**, 515–526
11 Conibear, P. B. and Geeves, M. A. (1998) Cooperativity between the two heads of rabbit skeletal muscle heavy meromyosin in binding to actin. Biophys. J. **75**, 926–937
12 Berger, C. E., Fagnant, P. M., Heizmann, S., Trybus, K. M. and Geeves, M. A. (2001) ADP binding induces an asymmetry between the heads of unphosphorylated myosin. J. Biol. Chem. **276**, 23240–23245
13 Stafford, W. F., Jacobsen, M. P., Woodhead, J., Craig, R., O Neall-Hennessey, E. and Szent-Györgyi, A. G. (2001) Calcium-dependent structural changes in scallop heavy meromyosin. J. Mol. Biol. **307**, 137–147
14 Spudich, J. A. and Watt, S. (1971) The regulation of rabbit skeletal muscle contraction. I. Biochemical studies of the interaction of the tropomyosin-troponin complex with actin and the proteolytic fragments of myosin. J. Biol. Chem. **246**, 4866–4871
15 Criddle, A. H., Geeves, M. A. and Jeffries, T. (1985) The use of actin labelled with N-(1-pyrenyl)iodoacetamide to study the interaction of actin with myosin subfragments and troponin/tropomyosin. Biochem. J. **232**, 343–349
16 Kurzawa, S. E. and Geeves, M. A. (1996) A novel stopped-flow method for measuring the affinity of actin for myosin head fragments using microgram quantities of protein. J. Muscle Res. Cell Motil. **17**, 669–676
17 Goody, R. S. and Holmes, K. C. (1983) Crossbridges and the mechanism of muscle contraction. Biochim. Biophys. Acta **728**, 13–39
18 Kurzawa-Goertz, S. E., Perreault-Micale, C. L., Trybus, K. M., Szent-Györgyi, A. G. and Geeves, M. A. (1998) Loop I can modulate ADP affinity, ATPase activity, and motility of different scallop myosins. Transient kinetic analysis of S1 isoforms. Biochemistry **37**, 7517–7525
19 Hill, T. L. (1978) Binding of monovalent and divalent myosin subfragments onto sites on actin. Nature (London) **274**, 825–826
20 Hill, T. L. and Eisenberg, E. (1980) Theoretical consideration in the equilibrium binding of myosin fragments on F-actin. Biophys. Chem. **11**, 271–281
21 Cremo, C. R. and Geeves, M. A. (1998) Interaction of actin and ADP with the head domain of smooth muscle myosin: implications for strain-dependent ADP release in smooth muscle. Biochemistry **37**, 1969–1978

Received 30 September 2002/18 November 2002; accepted 20 November 2002
Published as BJ Immediate Publication 20 November 2002, DOI 10.1042/BJ20021519